Ab Initio Electron Transport Study of Carbon and Boron−Nitrogen Nanowires

X. Q. Shi, Z. X. Dai, X. H. Zheng, and Z. Zeng*

Key Laboratory of Materials Physics, Institute of Solid State Physics, Chinese Academy of Sciences, Hefei 230031, China, and Graduate School of the Chinese Academy of Sciences, Beijing 100049, China

Received: December 20, 2005; In Final Form: May 6, 2006

We report first-principles calculations on the electrical transport properties of two kinds of one-dimensional nanowires: (a) a carbon nanowire (CNW) with alternating single and triple bonds and (b) a boron−nitrogen nanowire (BNNW) with equidistant bonds. We demonstrate the similarity and difference between the carbon nanowire and its boron−nitrogen analogue in the molecular orbital and transport properties, and then explore the potential innovations. The effects of molecular orbitals and nanowire-electrode coupling on the transport properties are analyzed. The cases of the nanowires sandwiched between both nanoscale and bulk electrodes are considered. It suggests that the characteristics of the transmission spectra and the current−voltage characteristics ($I-V$ curves) are determined both by the electrodes and by the molecule as well as their coupling. In particular, the negative differential resistance (NDR) phenomenon is more apparent when the nanowires are positioned between two nanoscale electrodes. The tuning of the transport properties is also probed through the changes of nanowire−electrode separation and the inclusion of a gate voltage. These lead to dramatic variations in the equilibrium conductance, which can be understood from the shift and alignment of the molecular orbital relative to the Fermi level of the electrodes. In the analysis of the effects of nanowire−electrode separation, it shows that the equilibrium conductance has the same variation behavior as that of the projected density of states (PDOS) for CNW, while the localized molecular orbitals of BNNW result in its conductance varies differently from its PDOS. The different molecular orbital characteristics near the Fermi level of these two kinds of nanowires underlie their different transport properties.

I. Introduction

Molecular electronics has attracted increasing interest both for fundamental reasons and for potential applications because it represents the ultimate miniaturization of electronic systems.[1] Much attention has been devoted to atomic-scale devices, and thus the transport properties of wire-like structures (such as gold, aluminum, and carbon one-dimensional nanowires) sandwiched between two metallic electrodes have been widely investigated.[2] Although their structures are simple, atomic-sized wires have shown peculiar transport properties due to their low dimensionality. In particular, the transport properties are strongly affected by the nature of single chemical bonds and the number of atoms.[3]

Carbon nanowires (CNWs) have been the subjects of many studies.[3−8] In particular, Lagow et al. have prepared CNWs with alternating single and triple bonds,[4] while the experimental evidence for CNWs is controversial and its properties are not completely known.[8] Some researchers demonstrated CNWs with alternating single and triple bonds, while others proposed CNWs with equidistant double bonds. Ab initio many-body calculations by Abdurahman et al. showed that CNWs exhibit bond-length alternation with alternating single and triple bonds, while boron−nitrogen nanowires (BNNWs) have strictly linear geometry and exhibit equidistant bonds.[6]

Most theoretical works for transport calculations of CNWs performed so far have treated CNWs with equidistant bonds.[3,7] Kushmerick et al. proposed that bond-length alternation plays an important role in determining the conductivity through the study of the transport properties of oligo phenylene ethynylene (OPE) and oligo phenylene vinylene (OPV) molecular wires.[9] Thus it is interesting to know whether bond-length alternation of CNW will decrease the conductivity when it is coupled with two metallic electrodes. Côté et al. proposed that there are some good qualities using boron nitride polymers as building blocks for electronic devices,[10] such as band gap tuning. Hence, the parallel investigation on the transport properties of BNNW and CNW may provide potential innovations. There appears to be a one-to-one correspondence between structures of carbon and boron−nitrogen allotropes in nature, and BNNWs are isoelectronic with CNWs. Thus if these two kinds of nanowires exhibit different transport properties, it will be due to the differences in the nature of bonding caused by different atomic species.

In the current work, the electrical transport properties of CNW and BNNW are analyzed from the total transmission spectra and its eigenchannel decompositions,[11] the characteristics of the isolated molecular orbitals, the current−voltage characteristics, and the zero-bias conductance at different nanowire−electrode distances as well as the nanowires subjected to a gate voltage to tune the magnitude of the conductivity. It is found that the transport properties are determined both by the molecular orbitals of the nanowires and by the electrodes. What interests us is that the gate voltage drastically increases the equilibrium conductance of BNNW. The different molecular orbital structures near the Fermi level of these two kinds of nanowires underlies the different transport properties.

This paper is organized as follows: In section II we give a brief description of the calculation method and the simulation model. Section III shows the detailed analysis of the electrical transport properties of these two kinds of nanowires sandwiched

* Address correspondence to this author. E-mail: zzeng@theory.issp.ac.cn.

10.1021/jp057396r CCC: $33.50
Published on Web 08/10/2006

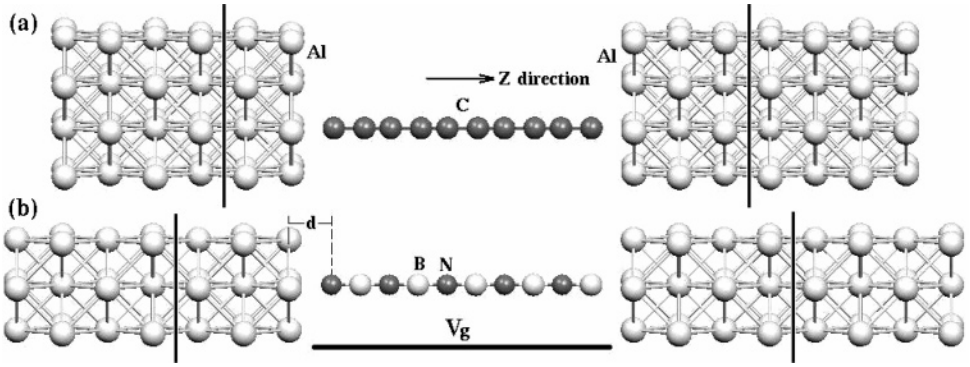

Figure 1. The simulation model of the nanowires coupled to (a) Al(100)−($2\sqrt{2} \times 2\sqrt{2}$) bulk electrodes and (b) Al(100) nanoscale electrodes. The region within two black lines is the scattering region and the remaining parts are the left and right electrodes. The aluminum electrodes extend to $z = \pm\infty$. The black bar with V_g above it denotes the gate voltage.

between both nanoscale and bulk electrodes. The effects of the molecular orbitals and nanowire−electrode coupling on the characteristics of transmission spectra and the $I-V$ curves are analyzed. The tuning of the equilibrium conductance through the changes of nanowire−electrode separation and the inclusion of a gate voltage is also presented. A brief summary is given in section IV.

II. Calculation Method and Simulation Model

The TranSIESTA-C package is used in the present work to study the transport properties of two-probe systems. TranSIESTA-C combines the well-tested electronic structure calculation method SIESTA[12] and the Keldysh NEGF (nonequilibrium Green's function) technique[13] to simulate electrical transport in molecular devices. The principles and the technique details of this method can be found in the listed references.[14]

Figure 1 shows the simulation models: a nanowire sandwiched between (a) two bulk electrodes and (b) two nanoscale electrodes. In model b we have chosen a supercell with a large enough vacuum layer in the x and y directions so that the device has no interaction with its mirror images. The sandwiched nanowire could be CNW or BNNW in our calculations and only either case is shown in Figure 1. In the calculations, the whole system is divided into three parts: the scattering region and the left and right electrodes. The nanowire together with several layers of surface atoms in the left and right that interact with the molecule are chosen as the scattering region and the remaining parts are regarded as the left and right semiinfinite electrodes (see Figure 1). The terminate atoms of the nanowires are positioned symmetrically above the Al(100) hollow sites. Without specializing, the nanowire−electrode separation d is 1.9 Å (ref 7a). The bond lengths of CNW and BNNW come from ref 6, i.e. 1.360 Å for the single bonds and 1.174 Å for the triple bonds in CNW, and 1.287 Å for the equidistant bonds in BNNW.

The system subjected to an external bias is highly in nonequilibrium. The left- and right-moving carriers have significantly different chemical potentials, and the electrostatic potential is a function of position in the molecule. Therefore, a full self-consistency method to describe the system is necessary. In the TranSIESTA-C code, a full self-consistency procedure of the electronic structure of the scattering region is performed before the transmission function and the current is calculated under each bias voltage. The electronic structure of the two electrodes is computed only once before the self-consistency procedure of the scattering region starts, and the self-consistent potential in the electrodes will be shifted rigidly relative to each other by the external voltage biases.[15] A SIESTA localized basis set is used to expand the valance electron wave functions and the core electrons are modeled by standard nonlocal norm conserving pseudopotential.[16] To calculate the electrostatic potential distribution (Kohn−Sham potential) in the scattering region, the electron density is required, and it is calculated by the density matrix that is constructed via NEGF technique.[13] The potential in the semiinfinite electrodes provides natural real space boundary conditions for the Kohn−Sham potential of the scattering region. The coupling of the scattering region with the electrodes is taken into account by self-energies. The Kohn−Sham potential includes contributions from Hartree, exchange, correlation, atomic core, and any other external potentials. This procedure is iterated until the convergence criterion 10^{-4} is achieved for the Hamiltonian, charge density, and band structure energy.

III. Results and Discussions

Figure 2 shows the total transmission spectra (T_t) and its eigenchannel decompositions (T_1 and T_2) of $C_{10}/(BN)_5$ sandwiched between two Al(100) nanoscale/bulk electrodes. The energy is relative to the average Fermi level of the two-probe system, i.e. $(\mu_l + \mu_r)/2$, where μ_l and μ_r are the electrochemical potentials of the left and right electrodes, respectively. Numerically, the transmission eigenchannel is extracted from the decomposition of the total transmission coefficient by transmission matrix diagonalization.[11] The transmission eigenchannel reflects the coupling between the molecular orbitals and the band structure of the electrodes.[18] Several observations are in order. At first, there are two degenerate channels contributing to the total transmission. The maximum value of the total transmission of CNW is 2, while a much smaller value of BNNW is around 0.3. Second, the equilibrium conductance ($G = (2e^2/h)T(E=0)$) of CNW with bond length alternation in the current work is comparable to that of CNW with equidistant bonds as presented in the previous work (see ref 7a). Finally, the transmission energy regions (with energy regions $T(E) > 0$) and transmission energy intervals, i.e. $T(E) = 0$, are mainly determined by the electrodes in the systems studied here. The transmission intervals become smaller when nanowires are sandwiched between bulk electrodes.

It is necessary to figure out the factors that determine the transmission coefficients (denoted by T hereafter). In the following, the cause of the characteristics of T will be illustrated from the effects of molecular orbitals and nanowire−electrode coupling, respectively.

A. Effects of Molecular Orbitals. It is well-known that the characteristics of T are determined by both the electrodes and the nanowires as well as their cooperation.[17] HOMOs (highest

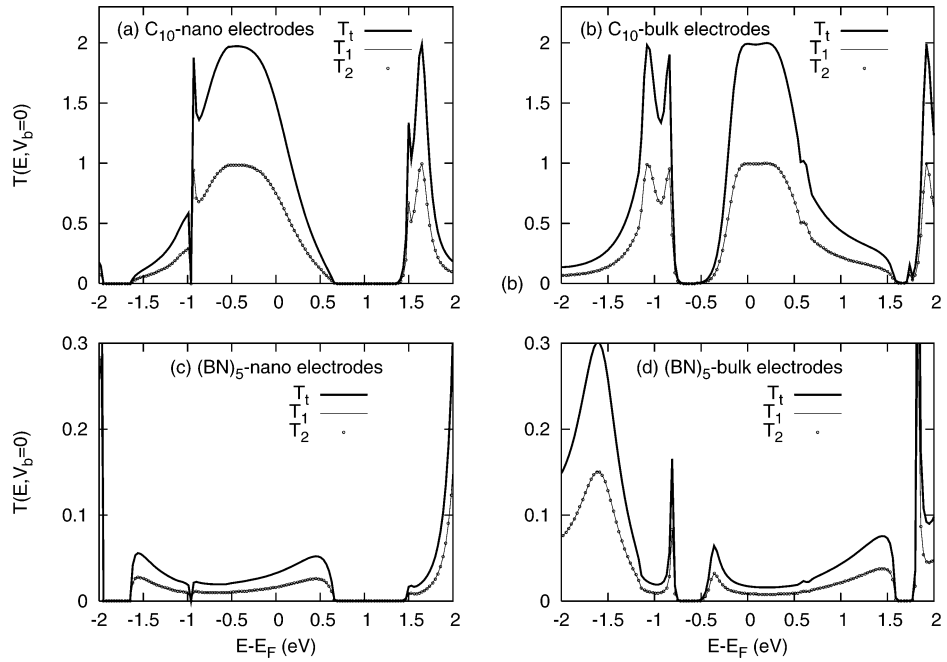

Figure 2. The total transmission spectra (T_t) and its eigenchannel decompositions (T_1 and T_2) of $C_{10}/(BN)_5$ sandwiched between two Al(100) nanoscale/bulk electrodes. C_{10} means 10 atoms of CNW and $(BN)_5$ means 10 atoms of BNNW. Note that only two channels contribute to the total transmission and they are equal.

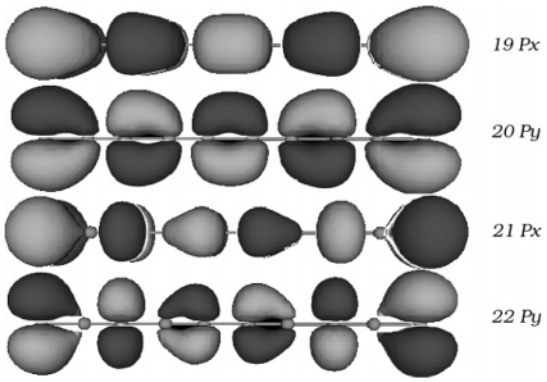

Figure 3. HOMOs (19 p_x and 20 p_y) and LUMOs (21 p_x and 22 p_y) of C_{10} nanowire with bond-length alternation. The HOMOs and the LUMOs are both composed of two degenerate π (p_x and p_y) orbitals which are spatially delocalized.

occupied molecular orbitals) and LUMOs (lowest unoccupied molecular orbitals) are very helpful tools for analyzing the transmission. Figure 3 shows the HOMOs and LUMOs of C_{10} with bond-length alternation, which are composed of two degenerate π (p_x and p_y) orbitals and are spatially delocalized. The two degenerate π (p_x and p_y) orbitals result in two degenerate channels contributing to the total transmission (see Figure 2a,b). The delocalized molecular orbitals cause the high transmission coefficients. The value of T reaches 2.0 in certain energy ranges, which means that these two channels are both entirely open. It is not the case for the $(BN)_5$ nanowire, however. The HOMOs of the $(BN)_5$ nanowire are composed of degenerate σ (sp_z) and π (p_x and p_y) orbitals, while the LUMOs are composed of two degenerate π (p_y and p_x) orbitals, as shown in Figure 4. The molecular orbitals are localized on either B or N due to the difference in ionicity of B and N, which result in a small transmission coefficient (see Figure 2c,d). Only two degenerate channels contribute to the total transmission implying only the two degenerate π (p_x and p_y) orbitals contribute to the transmission, while the σ (sp_z) orbital has no contribution to the total transmission.

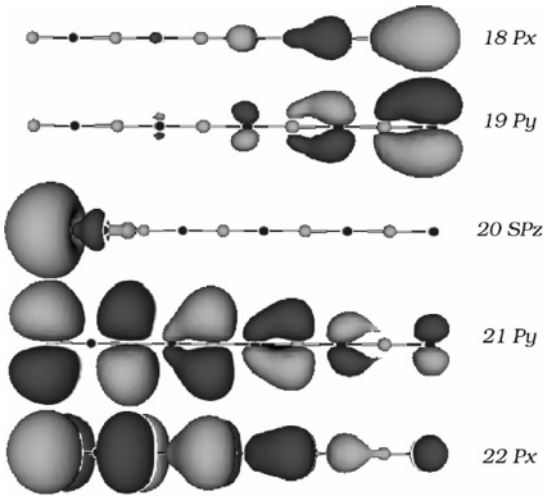

Figure 4. HOMOs (18 p_x, 19 p_y, and 20 sp_z) and LUMOs (21 p_y and 22 p_x) of $(BN)_5$ nanowire. The HOMOs are composed of degenerate σ (sp_z) and π (p_x and p_y) orbitals, which are spatially localized to the left or the right of the nanowire. The LUMOs are composed of two degenerate π (p_y and p_x) orbitals which are spatially delocalized. The orbitals are located on different atomic species (either B or N) due to the difference in ionicity of B and N.

One may wonder whether this difference is due to the symmetry difference between C_{10} and $(BN)_5$. We have also done a symmetric calculation for $(BN)_5B$, and found that the transmission remains very small (about 0.1 near Fermi level). The molecular orbitals of $(BN)_5B$ are still localized on either B or N.

B. Effects of Nanowire−Electrode Coupling. Calzolari et al. showed that the infinite CNW with bond-length alternation opens energy gaps at the edges of the Brillouin zone and the present semiconducting feature, while CNW with equidistant bonds displays metallic behavior (see ref 7b). Kushmerick et al. proposed that bond-length alternation will greatly decrease the conductivity through the comparison of the transport properties of OPE and OPV[9] molecular wires. However, in our calculation, when a C_{10} nanowire with bond-length alternation

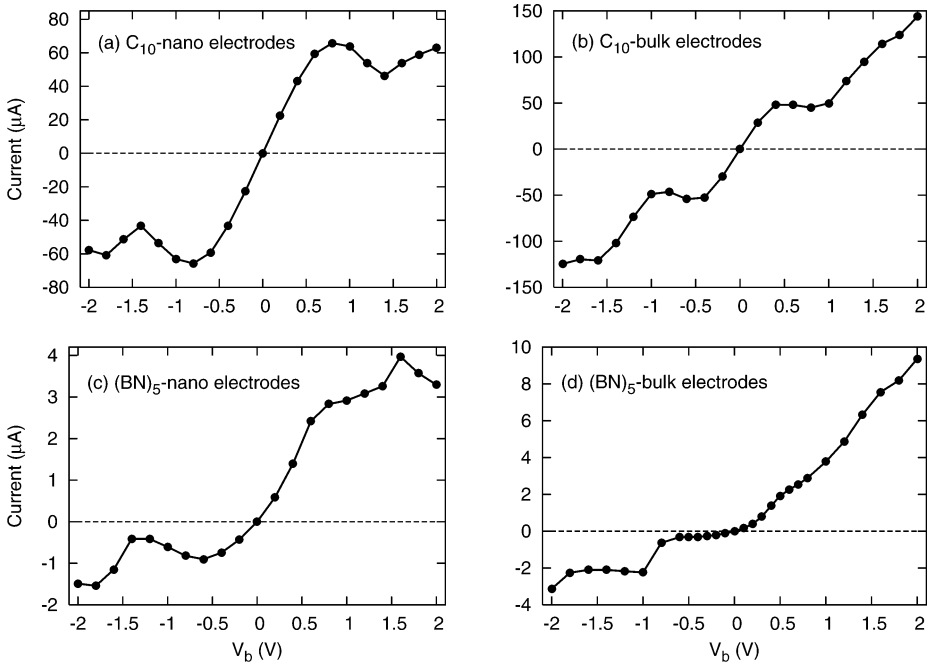

Figure 5. The $I-V$ curves of $C_{10}/(BN)_5$ sandwiched between two Al(100) nanoscale/bulk electrodes.

is sandwiched between two electrodes, the equilibrium conductance of 1.5 or 2.0 G_0 (see Figure 2a,b, where G_0 is the quantum conductance) is obtained, which is comparable to that of CNW with equidistant bonds sandwiched between two nanoscale electrodes (see ref 7a). The reason the conduction of CNW with bond-length alternation dose not decrease can be found from Lang and Avouris' works,[3] where they proposed that the bonding of the nanowire to the electrodes and the accompanying charge transfer doping could modify the conductivity of the nanowire. So the high conductance of CNW with bond-length alternation just comes from the nanowire−electrode coupling and the accompanying charge transfer doping. This can be clearly seen in the latter (see Figure 6 in subsection D).

Kaun et al. suggested that the characteristic of T is determined by the band structure of the electrodes and the momentum filtering effect of the nanowires,[18] which means that only those Bloch bands of the electrodes having the same orbital character as the molecular states near the Fermi level conduct well. In the present work, these two kinds of nanowires have a similar moment filtering effect, i.e., only Bloch bands with π orbital feature will conduct. Due to the similar moment filtering effect of these two kinds of nanowires, the transmission energy intervals seem insensitive to the nanowires and are determined by the band gaps of the electrodes. In fact, when a molecule with mainly σ orbitals is placed near the Fermi energy of the electrodes, the energy intervals will also be sensitive to the molecule.[18] The bulk electrodes contribute more to the bands with more Bloch states than the nanoscale electrodes do, which is the origin of the smaller transmission energy intervals when nanowires are sandwiched between bulk electrodes.

C. The $I-V$ Characteristics. Figure 5 shows the $I-V$ curves of the nanowires sandwiched between Al(100) electrodes. The current I is calculated by $I(V_b) = (2e/h)\int_{-\infty}^{+\infty} dE\,[f_l(E-\mu_l) - f_r(E-\mu_r)]T(E,V_b)$, where f_l/f_r is the electron distribution function of the left/right electrode. It can be seen that the $I-V$ characteristics are determined by both the nanowires and the electrodes, while the NDR (negative differential resistance, which is characterized by the decrease of current with the increase of the external bias) phenomenon is more apparent when the nanowires are sandwiched between nanoscale electrodes. The origin of NDR can be understood from the changes of coupling between the electrodes and the nanowire at various external biases as illustrated in detail in our previous work.[17] The $I-V$ curves are symmetric with respect to bias polarity for CNW due to the symmetric coupling of CNW with the left and right electrodes, while they are asymmetric for BNNW as the result of asymmetric coupling of BNNW with the left and right electrodes (see Figure 1, on the left, nitrogen atom bonding with the left electrode, while on the right, boron atom bonding with the right electrode). Specifically, the $I-V$ curves show metallic behavior at small biases when CNW is sandwiched between nanoscale electrodes as seen in Figure 5a, while a rectifying behavior appears when BNNW is sandwiched between bulk electrodes as presented in Figure 5d. The rectification ratio is about 7 at ± 0.6 eV obtained in this figure.

D. The Tuning of Transport Properties. Experimentally, people have the ability to adjust the spacing between the electrodes mechanically and the ability to shift the energy levels in the molecule using a gate electrode.[19] To further study the transport properties of these two kinds of nanowires and explore their differences, we investigate the tuning of the transport properties with the nanowires sandwiched between two nanoscale electrodes.

Figures 6a and 7a show the variation of the equilibrium conductance with nanowire−electrode separation d. As seen from Figure 6a, when d varies from 0.5 to 2.7 Å, the equilibrium conductance of CNW increases first. At $d = 2.1$ Å, the conductance reaches its maximum, which means that the two degenerate transmission eigenchannels are fully open. Then, the zero-bias conductance decreases as d increases further. For BNNW, the equilibrium conductance decreases monotonically, as shown in Figure 7a.

We may understand the variation of the conductance with d from the shift and alignment of the molecular orbitals relative to the Fermi level of the electrodes. Figures 6b and 7b show the charge transfer from the electrodes to the nanowire. With the increase of d, the charge transfer from the electrodes to the nanowire decreases monotonically, which means that the molecular orbitals shift up with respect to the Fermi level of the electrodes. For CNW, the upshift of the molecular orbitals

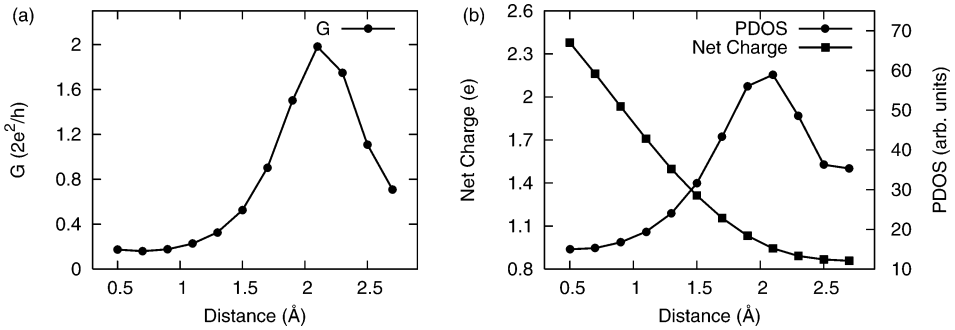

Figure 6. (a) The equilibrium conductance G of C_{10} as a function of d and (b) the corresponding PDOS at the Fermi level and charge transfer from the electrode to the C_{10} nanowire.

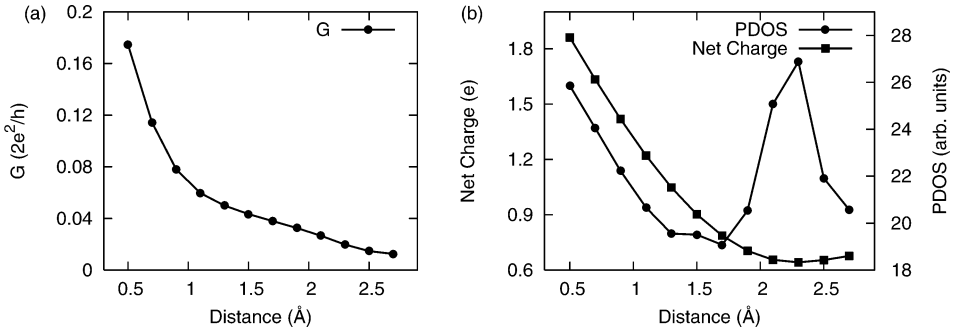

Figure 7. (a) The equilibrium conductance G of $(BN)_5$ as a function of d and (b) the corresponding PDOS at the Fermi level and charge transfer from the electrode to the $(BN)_5$ nanowire.

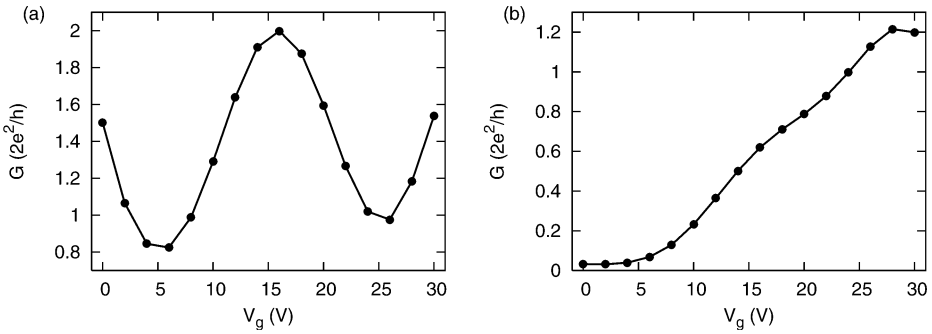

Figure 8. The equilibrium conductance G of (a) C_{10} and (b) $(BN)_5$ as a function of gate voltage.

relative to the Fermi level of the electrodes will cause an oscillatory conductance. When an energy level of CNW aligns with the Fermi level of the electrodes, a conductance peak appears. With the further upshift of the molecular orbitals, the conductance decreases. However, for BNNW, the upshift of the molecular orbitals means that the spatially localized HOMOs move toward the Fermi level of the electrodes, and this causes the decrease of the conductance.

It is well-known that only delocalized states contribute to the conductance significantly. To compare the equilibrium conductance with the density of states of the nanowire, Figures 6b and 7b also show the projection of the density of states (PDOS) of the two-probe system onto all the basis orbitals of the nanowire. Since the equilibrium conductance is the transmission at the Fermi energy, only the PDOS at the Fermi energy is needed. The PDOS is given by $P(E) = \langle \psi^{w}(E)|\Psi(E)\rangle = \langle \sum_i^{\text{wire}} c_i(E)\phi_i(\vec{r})|\sum_j^{\text{all}} c_j(E)\phi_j(\vec{r})\rangle$, where $\Psi(E)$ is the eigenstate of the whole system and $\psi^{w}(E)$ is the contribution of the basis orbitals of the nanowire to $\Psi(E)$, $\{\phi\}$ are the nonorthogonal basis sets of the system, and c_i and c_j are expanding coefficients. The sum over i runs over the basis orbitals of the molecule and the sum over j runs over all the basis orbitals of the whole system. From Figures 6 and 7 we see that the equilibrium conductance G has the same variation behavior as that of PDOS in CNW since its orbitals are delocalized, while the localized molecular orbitals of BNNW result in its conductance varying differently from its PDOS. The difference in how G responses to the PDOS comes from the different orbitals of CNW and BNNW, and it is a pure effect from the different nature of bonding between these two kinds of nanowires.

Figure 8 shows the tuning of the transport behavior of both CNW and BNNW through the inclusion of a gate voltage. We simulate the electrostatic effect of the gate electrode by shifting the Hamiltonian of the nanowire part with the gate voltage, and then solve the potential in the central region self-consistently. This corresponds to assuming that the gate electrode induces an external potential localized to the molecular region. For metallic electrodes this will be a reasonable approximation.[14,20] The gate voltage drastically increases the equilibrium conductance of BNNW, which can also be understood from the shift and alignment of the molecular orbitals relative to the Fermi level of the electrodes. Here, the positive gate voltage means the downshift of the energy levels in the nanowire relative to the Fermi level of the electrodes.[21] For CNW, the equilibrium conductance shows an oscillatory behavior as Figure 6a. However, for BNNW, due to the downshift of the energy levels, spatially delocalized LUMOs move close to the Fermi level of the electrodes, which is the origin of the increase of the

conductance. With the increases of the gate voltage, BNNW switches from a weakly conducting to a highly conducting state continuously, which indicates that it might be a good candidate for molecular switch.

IV. Conclusion

In summary, the transport properties of CNW and BNNW sandwiched between Al(100) electrodes have been studied. The effects of the characteristics of the molecular orbitals and the effects of the nanowire−electrode coupling on the transport properties are analyzed. Only two degenerate transmission eigenchannels contribute to the total transmission. The NDR phenomenon is more apparent when the nanowires are sandwiched between nanoscale electrodes. A rectifying phenomenon appears when BNNW is sandwiched between bulk electrodes. The current−voltage curves are asymmetric with respect to bias polarity for BNNW due to asymmetrical coupling of BNNW with the left and the right electrodes. With the changes of nanowire−electrode separation d the conductance has the same variation behavior as that of PDOS in CNW, while the localized molecular orbitals of BNNW result in its conductance varying differently from its PDOS. A positive gate voltage switches BNNW from a weakly conducting to a highly conducting state continuously. The variation of the equilibrium conductance with the changes of d or the inclusion of the gate voltage can be understood from the shift and alignment of the molecular orbitals relative to the Fermi level of the electrodes. Both switching and rectifying phenomena are predicated for BNNW, which means that it might be a good candidate for a molecular device.

Acknowledgment. This work was supported by the National Science Foundation of China under Grant No. 10374091, Knowledge Innovation Program of Chinese Academy of Sciences, and Director Grants of Hefei Institutes of Physical Sciences. Part of the calculations were performed in the Center for Computational Science, Hefei Institutes of Physical Sciences.

References and Notes

(1) Heath, J. R.; Ratner, M. A. *Phys. Today* **2003**, *56*, 43. Nitzan, A.; Ratner, M. A. *Science* **1384**, *300*, 2003.

(2) Agraït, N.; Levy Yeyati, A.; van Ruitenbeek, J. M. *Phys. Rep*. **2003**, *377*, 81 and references therein.

(3) Lang, N. D.; Avouris, Ph. *Phys. Rev. Lett*. **1998**, *81*, 3515; **2000**, *358*, *84*.

(4) Lagow, R. J.; Kampa, J. J.; Wei, H.-C.; Battle, S. L.; Genge, J. W.; Laude, D. A.; Harper, C. J.; Bau, R.; Stevens, R. C.; Haw, J. F.; Munson, E. *Science* **1995**, *267*, 362.

(5) Zhao, X.; Ando, Y.; Liu, Y.; Jinno, M.; Suzuki, T. *Phys. Rev. Lett*. **2003**, *90*, 187401.

(6) Abdurahman, A.; Shukla, A.; Dolg, M. *Phys. Rev. B* **2002**, *65*, 115106.

(7) (a) Larade, B.; Taylor, J.; Mehrez, H.; Guo, H. *Phys. Rev. B* **2001**, *64*, 075420. (b) Calzolari, A.; Marzari, N.; Souza, I.; Nardelli, M. B. *Phys. Rev. B* **2004**, *69*, 035108. (c) Tongay, S.; Senger, R. T.; Dag, S.; Ciraci, S. *Phys. Rev. Lett.* **2004**, *93*, 136404. (d) Senger, R. T.; Tongay, S.; Dag, S.; Durgun, E.; Ciraci, S. *Phys. Rev. B* **2005**, *71*, 235406. (e) Ke, S.; Baranger, H. U.; Yang, W. T. *Phys. Rev. B* **2005**, *71*, 113401. (f) Wang, B.; Xing, Y. X.; Wan, L. H.; Wei, Y. D.; Wang, J. *Phys. Rev. B* **2005**, *71*, 233406.

(8) Kavan, L. *Carbon* **1998**, *36*, 801. Ravagnan, L.; Siviero, F.; Lenardi, C.; Piseri, P.; Barborini, E.; Milani, P.; Casari, C. S.; Li Bassi, A.; Bottani, C. E. *Phys. Rev. Lett*. **2002**, *89*, 285506.

(9) Kushmerick, J. G.; Holt, D. B.; Pollack, S. K.; Ratner, M. A.; Yang, J. C.; Schull, T. L.; Naciri, J.; Moore, M. H.; Shashidhar, R. *J. Am. Chem. Soc*. **2002**, *124*, 10654.

(10) Côté, M.; Haynes, P. D.; Molteni, C. *Phys. Rev. B* **2001**, *63*, 125207.

(11) Brandbyge, M.; Sørensen, M. R.; Jacobsen, K. *Phys. Rev. B* **1997**, *56*, 014956.

(12) Soler, J. M.; Artacho, E.; Gale, J. D.; Garcia, A.; Junquera, J.; Ordejón, P.; Sanchez-Portal, D. *J. Phys.*: *Condens. Matter* **2002**, *14*, 2745.

(13) Jauho, A.-P.; Wingreen, N. S.; Meir, Y. *Phys. Rev. B* **1994**, *50*, 5528. Haug, H.; Jauho, A.-P. *Quantum Kinetics in Transport and Optics of Semiconductors*; Springer-Verlag: Berlin, Germany, 1996.

(14) Brandbyge, M.; Mozos, J.-L.; Ordejón, P.; Taylor, J.; Stokbro, K. *Phys. Rev. B* **2002**, *65*, 165401. Taylor, J.; Guo, H.; Wang, J. *Phys. Rev. B* **2001**, *63*, 245407. Taylor, J.; Ph.D. Thesis, McGill University, 2000. The software is provided by the Atomistix Corp.

(15) Stokbro, K.; Taylor, J.; Brandbyge, M.; Mozos, J.-L.; Ordejón, P. *Comput. Mater. Sci.* **2003**, *27*, 151.

(16) Hamann, D. R.; Schlüter, M.; Chiang, C. *Phys. Rev. Lett*. **1982**, *43*, 1494.

(17) Shi, X. Q.; Zheng, X. H.; Dai, Z. X.; Wang, Y.; Zeng, Z. *J. Phys. Chem. B* **2005**, *109*, 3334.

(18) Kaun, C.-C.; Guo, H.; Grütter, P.; Lennox, R. B. *Phys. Rev. B* **2004**, *70*, 195309.

(19) Champagne, A. R.; Pasupathy, A. N.; Ralph, D. C. *Nano Lett*. **2005**, *5*, 305.

(20) Atomistix, http://www.atomistix.com, TranSIESTA-C Manual: Tutorial and User's Guide.

(21) Datta, S. *Nanotechnology* **2004**, *15*, S433.